JOURNAL OF APPLIED PHYSICS 109, 063913 (2011)

Epitaxial integration of photoresponsive $Bi_{0.4}Ca_{0.6}MnO_3$ with Si(001)

Grace J. Yong,[1,a] Rajeswari M. Kolagani,[1,a] Benjamin P. Hofmann,[1] Sanjay Adhikari,[1] Yong Liang,[2] and Vera N. Smolyaninova[1,a]
[1]*Department of Physics, Astronomy and Geosciences, Towson University, 8000 York Rd., Towson, Maryland 21252, USA*
[2]*Motorola Inc., 2900 S. Diablo Way, Bldg. A Suite 150, Tempe, Arizona 85282, USA*

(Received 19 August 2010; accepted 2 February 2011; published online 24 March 2011)

Previously it has been shown that the resistivity of $Bi_{0.4}Ca_{0.6}MnO_3$ epitaxial thin films on oxide substrates decreases significantly upon illumination with visible light. The resistivity decrease is observed over a wide temperature range and is understood as arising due to the destruction of charge ordering. The light responsivity makes $Bi_{0.4}Ca_{0.6}MnO_3$ thin films attractive for photonic and optoelectronic device applications. In this paper, we report the heteroepitaxy of $Bi_{0.4}Ca_{0.6}MnO_3$ thin films on (001) Si which is relevant for the potential integration of the optoelectronic/photonic functionality of $Bi_{0.4}Ca_{0.6}MnO_3$ with semiconductor electronics. As in the case of other perovskite oxides, heteroepitaxy of $Bi_{0.4}Ca_{0.6}MnO_3$ on Si requires the use of buffer layers to circumvent the problems associated with the presence of an amorphous native silicon dioxide layer and the reactivity of perovskite oxides with Si at high temperatures. We demonstrate that high quality epitaxial thin films of $Bi_{0.4}Ca_{0.6}MnO_3$ can be grown via pulse laser deposition on Si that has been prebuffered with a $SrTiO_3$ layer via a Motorola molecular beam epitaxy process. The magnitude and dynamics of the photoresponse in these films is comparable to that of $Bi_{0.4}Ca_{0.6}MnO_3$ films on oxide substrates. © *2011 American Institute of Physics*. [doi:10.1063/1.3561371]

I. INTRODUCTION

Permanent photoinduced reflectivity changes were observed in a charge ordered (CO) $Bi_{0.3}Ca_{0.7}MnO_3$ single crystal, and the potential of this phenomenon for creation of various photonic materials was demonstrated.[1] In bulk $Bi_{0.4}Ca_{0.6}MnO_3$, the CO transition occurs at 330 K and is accompanied by a structural transition with a sharp increase in the a and b (a = b) lattice parameters and a sharp decrease in the c lattice parameter. Such changes provide the lattice distortions necessary for existence of the CO phase. Lattice parameters in the CO state just below 330 K are a = b = 3.81 Å, c = 2 × 3.79 Å and in the charge disordered state just above 330 K are a = b = 3.83 Å, c = 2 × 3.77 Å.[2] Since visible light penetrates into the bulk of this material only to a depth of about 3000 Å,[1] it is conceivable that thin films of $Bi_{1-x}Ca_xMnO_3$ with CO at room temperature may be suitable for photonic applications. This was the motivation for subsequent work performed on epitaxial $Bi_{1-x}Ca_xMnO_3$ on various oxide substrates, mostly with the composition $Bi_{0.4}Ca_{0.6}MnO_3$ due to its ~330 K CO transition temperature (slightly above room temperature). Work on $LaAlO_3$, $SrTiO_3$, and $NdCaAlO_4$ substrates showed that, upon illumination with visible light, the resistivity of $Bi_{0.4}Ca_{0.6}MnO_3$ epitaxial thin films on oxide substrates decreases significantly in a wide temperature range due to the destruction of CO. It would be very useful to have such thin films on Si substrates since Si is a material of choice for modern optoelectronics. Epitaxial growth on Si also opens up the possibility of fabricating a free-standing, strain-free $Bi_{0.4}Ca_{0.6}MnO_3$ membrane via standard Si micromachining techniques[3] with properties close to single crystals, where permanent photoinduced changes were observed.[1]

II. EXPERIMENT

Although Si(001) provides a good lattice match for manganites (see Fig. 1), direct pulse laser deposition (PLD) epitaxial growth of manganites on silicon is not possible due to reactivity. However, many groups have demonstrated high quality epitaxial (001) oriented $SrTiO_3$ grown by various molecular beam epitaxy (MBE) processes.[4] For our epitaxial $Bi_{0.4}Ca_{0.6}MnO_3$ growth, we used Si(001) that had a 100 Å high quality epitaxial (001) oriented layer of $SrTiO_3$ deposited by MBE at Motorola.[5] The Motorola MBE process involves temperature and pressures ranging from ~400 °C and 1×10^{-8} Torr O_2 at the early stage to 550 °C and 2×10^{-7} Torr O_2 at the later stage of growth. First, the original amorphous native SiO_2 layer on the Si wafer is removed/converted to a crystalline, silicate-like, pseudomorphic (and possibly two-dimensional) Sr_2SiO_4 template layer by a flux of Sr(g).[6] Then, Sr(g) and Ti(g) fluxes are co-deposited, and when O_2(g) is added, the $SrTiO_3$ film is grown. During the growth of the $SrTiO_3$ film, the template layer undergoes changes and an amorphous interlayer (AIL) develops. Growth of the AIL occurs via O_2 diffusion (O_2 pressure of 1×10^{-8} to 2×10^{-7} Torr) to the Si-SiO_2 interface (to a diffusion limited thickness of ~30 Å) and does not interfere with the epitaxy of the $SrTiO_3$ layer. Figure 2 shows a TEM cross section of a 55 Å high quality epitaxial (100) oriented layer of $SrTiO_3$ (thinner but made with the same Motorola MBE process) in which it can be seen that the AIL has reached a thickness of ~25 Å and that the epitaxy of the 55 Å $SrTiO_3$ is

[a]Authors to whom correspondence should be addressed. Electronic addresses: GYong@towson.edu, RKolagani@towson.edu and VSmolyaninova@towson.edu.

 © 2011 American Institute of Physics

Downloaded 18 Apr 2011 to 129.2.19.99. Redistribution subject to AIP license or copyright; see http://jap.aip.org/about/rights_and_permissions

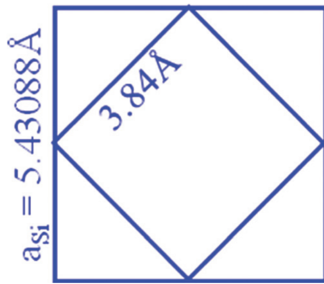

FIG. 1. (Color online) Schematic of the lattice match provided by the Si unit cell for the manganite pseudocubic unit cell.

intact. The AIL is understood to be a mixture of Sr-silicates ($SrSiO_3$, Sr_2SiO_4, Sr_3SiO_5) and SiO_x species (including SiO, Si_2O_3, SiO_2).[6,7] Any subsequent heating in significant O_2 partial pressure (e.g., the PLD process) causes further thickening of the AIL via the production of mostly SiO_2.

Before our PLD deposition, the MBE $SrTiO_3$ buffered Si(001) substrate was cleaned for 5 min each in trichloroethylene, acetone, and methanol with ultrasonic agitation. The substrate was mounted with a Ag paste (fixed with a 200 °C anneal) to the PLD heater block after which the heating block assembly with the substrate was placed into the PLD chamber and the pressure was reduced to $< 1.5 \times 10^{-5}$ Torr. A commercial 248-nm KrF pulsed excimer laser (COMPEX 205) with 25 ns pulse duration and a fluence of ~2 J/cm^2 was used with target-to-substrate distance of 8.5 cm. We explored two slightly different approaches for the heteroepitaxy of $Bi_{0.4}Ca_{0.6}MnO_3$ on Si, both of which employ a Motorola silicon substrate prebuffered with a 100 Å layer of $SrTiO_3$ grown by MBE.[5] In the first approach, the $Bi_{0.4}Ca_{0.6}MnO_3$ layer was directly deposited on the prebuffered substrates. In the second approach, additional $SrTiO_3$ was deposited by PLD on the MBE buffer layer, followed by the deposition of the $Bi_{0.4}Ca_{0.6}MnO_3$ layer. Commercial targets with nominal composition $Bi_{0.4}Ca_{0.6}MnO_x$ (BCMO) and $SrTiO_x$ (STO) were mounted on a rotating carousel in the PLD chamber (Neocera Inc.). Before all depositions, the chamber was pumped down to a base pressure $< 1.5 \times 10^{-5}$ Torr before it was backfilled with O_2 gas to the O_2 pressure required for the first deposition layer (400 mTorr for BCMO and 1×10^{-3} Torr for the STO). In the first preliminary type of samples, the heater block with the mounted Motorola MBE substrate was heated to various temperatures (790, 780, 770, 760, 750, and 740 °C) so as to optimize the BCMO layer deposition temperature. In the second type of samples, the heater block was first heated to 600 °C for the STO deposition. 20,000 pulses of STO were deposited at 10 Hz, resulting in a final total thickness of ~8500 Å STO. Then, the O_2 pressure was increased to 400 mTorr and temperature was ramped up to 750 °C for the BCMO deposition. 6,000 pulses of BCMO were deposited at 10 Hz, resulting in a final thickness of ~375 Å BCMO. In both types of samples, after the final BCMO layer was deposited, the chamber was backfilled with [mt]400 Torr O_2, and the samples were cooled to room temperature at 1 °C/min.

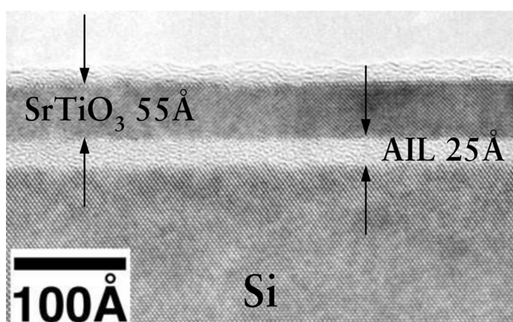

FIG. 2. TEM of as grown Motorola MBE epitaxial (001) oriented $SrTiO_3$ on Si(001). The $SrTiO_3$ layer of this sample is 55 Å and the AIL is ~25 Å.

X-ray scans were performed using a high resolution four-circle x-ray diffractometer in parallel beam geometry with a Göbel mirror and Soller slit (Bruker AXS model Discover D8).

For photoresponse studies, direct current resistivity was measured by a four-probe method using a four-in-line electrical contact configuration (see Fig. 7 inset). The distance between voltage contacts was approximately 0.3 mm. The space between voltage contacts was illuminated with full power (150 mW) multiwavelength (514, 488, 476, and 457 nm) argon laser light. Data were taken while the sample temperature was ramped up at a rate of 2 K/min. The time dependence of the photoinduced resistance changes was examined by fixing the temperature and measuring the resistance as the illumination was switched on and then off.

III. RESULTS AND DISCUSSION

A. Optimizing film growth conditions

Initially, the deposition temperature of 790 °C was selected as a reasonable growth temperature since good BCMO films have previously been obtained at 800 °C on oxide substrates[8–10] and $Nd_{0.67}Sr_{0.33}MnO_3$ films of good quality have previously been obtained at 780 °C on $SrTiO_3$ buffered Si(001) (Ref. 11) and at 790 °C on Si(001) using another buffer layer scheme.[12] However, for samples grown at 790 and 780 °C, x-ray 2θ–ω scans revealed that both the $BCMO(002)_{psuedocubic}$ and the STO(002) peaks were absent, while additional peaks indicative of reaction products were present (Fig. 3). The positions of these additional peaks are consistent with the presence of $SrSiO_3$ and $TiSi_2$ (Ref. 13), which was observed in an earlier study on the thermal stability of MBE $SrTiO_3$ layers on Si(001) substrates.[14] We also found that the samples grown at higher temperatures had significantly higher resistivity when compared to BCMO films on oxide substrates. As shown in Fig. 3, upon reducing the BCMO growth temperature from 790 to 750 °C, the BCMO $(002)_{psuedocubic}$ and STO(002) peaks progressively emerge and the extrinsic peaks corresponding to the reaction products progressively diminish. This is accompanied by a decrease in sample resistivity with decreasing growth temperatures. Interestingly, at 740 °C, the trend reverses with a reaction product peak returning and with the resistivity at 740 °C being higher than that of the film deposited at 750 °C. Also we see a pronounced shoulder on the low angle side of the BCMO $(002)_{psuedocubic}$ peak. This low angle shoulder is consistent with regions of oxygen deficient BCMO with

Downloaded 18 Apr 2011 to 129.2.19.99. Redistribution subject to AIP license or copyright; see http://jap.aip.org/about/rights_and_permissions

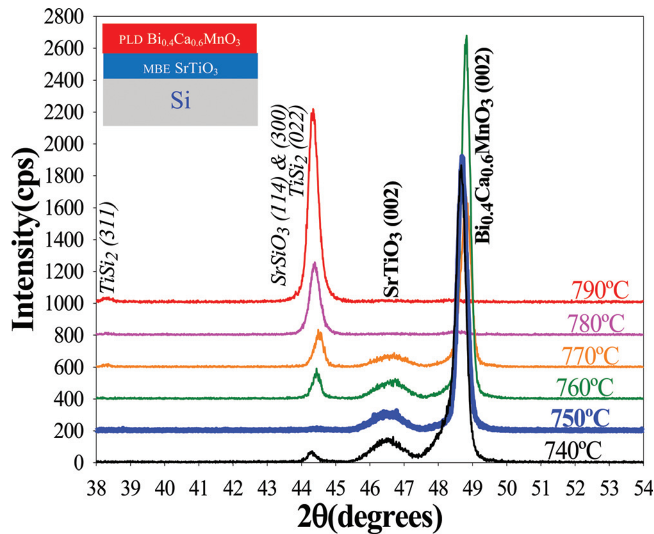

FIG. 3. (Color online) X-ray 2θ–ω scans of BCMO film growth at different deposition temperatures on Si(001) substrate prebuffered by MBE with 100 Å $SrTiO_3$. Inset shows the sequence of layers.

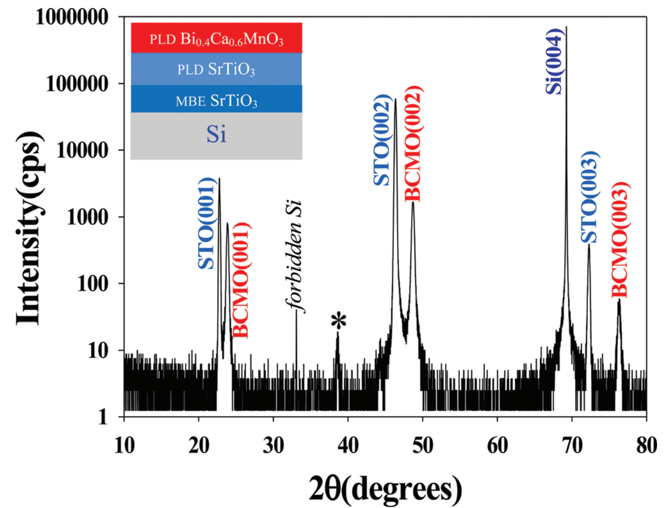

FIG. 4. (Color online) X-ray 2θ–ω scan of sample with extra $SrTiO_3$ deposited via PLD (total STO thickness ~8500 Å) showing c-axis aligned peaks (with very strong $SrTiO_3$ x-ray peaks). The asterisk (*) denotes a spurious peak from the anodized Al sample chuck. Inset shows the sequence of layers.

expanded lattice constant[15] which can be explained by reduced oxygen diffusivity at the lower growth temperature. In our study of the thermal stability of $SrTiO_3$ on Si, we found that oxygen transport across the interface is a mitigating factor restraining the degradation of the $SrTiO_3$ layer at high temperatures.[14] Thus, it is conceivable that the oxygen deficient BCMO layer in turn promotes increased reactivity of the $SrTiO_3$ layer with Si. The BCMO film deposited at 750 °C had the lowest resistivity of all the samples in Fig. 3. Thus, we selected 750 °C as our optimum growth temperature for the BCMO layer on $SrTiO_3$ buffered Si.

In our second growth scheme, we deposited a second much thicker layer of STO on the MBE 100 Å STO layer prior to the BCMO deposition. This was done as a precaution against any degradation of the STO template layer and also so as to ensure electrical isolation of the BCMO layer from the semiconducting Si (p-doped) substrate. (STO is an insulator when fully oxygenated.) As expected, x-ray 2θ–ω scan of this sample with an extra second layer of PLD STO has much stronger STO peaks when compared to that of the samples with only the MBE STO layer (compare Figs. 4 and 3). The rocking curve analysis of the STO(002) peak in Fig. 4 shows a 0.22° FWHM, indicating good crystallinity, and the STO(002) out of plane peak gives a lattice parameter of 3.914 Å, which is marginally larger than that of bulk STO (3.905 Å). This is indicative of significant strain relaxation in the STO layer. [For strained, unrelaxed STO, one would expect a larger out of plane lattice parameter; as seen in Fig. 1, the in-plane lattice constant provided by Si(001) for epitaxial perovskite growth is only 3.84 Å.] As an indicator of the accuracy of our measurements, the Si(004) out of plane peak gives a lattice parameter of 5.422 Å, which is marginally smaller than that of the expected value of 5.431 Å. The rocking curve analysis of the $BCMO(002)_{psuedocubic}$ peak shows a 0.407° FWHM, indicating a good crystallinity. The $BCMO(002)_{pseudocubic}$ out of plane peak gives a lattice parameter of 3.736 Å, which is smaller than that of bulk BCMO ($V^{1/3}$ ~3.81 Å) (Ref. 2), indicating that some tensile strain is present. This is consistent with the bulk BCMO lattice parameters a = b = 3.86 Å (Ref. 2) being smaller than the in-plane lattice parameter of strain relaxed STO of ~3.905 Å. φ scans were performed to confirm the in-plane alignment between the different layers. Figure 5 shows the schematics of the relative orientations expected for the different crystal planes selected for the φ scans. It is expected that the STO layer grows in the "diagonal-on-side" manner onto the Si template whereas the epitaxial BCMO growth occurs in a "cube-on-cube" manner on the STO. According to this expected epitaxial alignments, the BCMO $(101)_{psuedo\text{-}cubic}$ plane cuts across the surface perpendicular to the [001] direction along the $[110]_{Si}$ direction, the STO(101) plane cuts across the surface perpendicular to the [001] direction along the $[110]_{Si}$ direction, and the Si(202) plane cuts across the surface perpendicular to the [001] direction along the $[100]_{Si}$ direction. The measured φ scans are shown in Fig. 6.

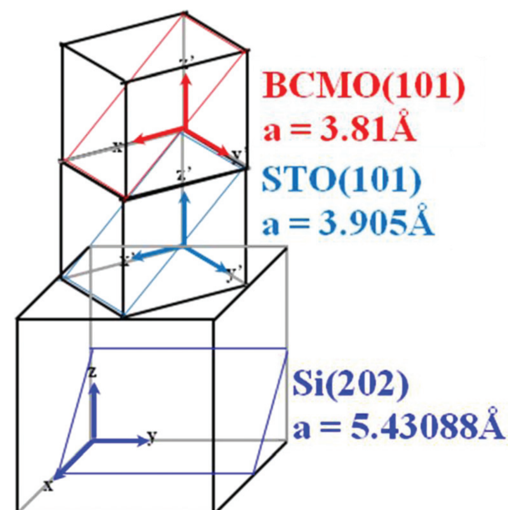

FIG. 5. (Color online) Schematic orientation of c-axis aligned, epitaxial layers of BCMO and STO on c-axis oriented Si (labeled with bulk values of lattice constants).

Downloaded 18 Apr 2011 to 129.2.19.99. Redistribution subject to AIP license or copyright; see http://jap.aip.org/about/rights_and_permissions

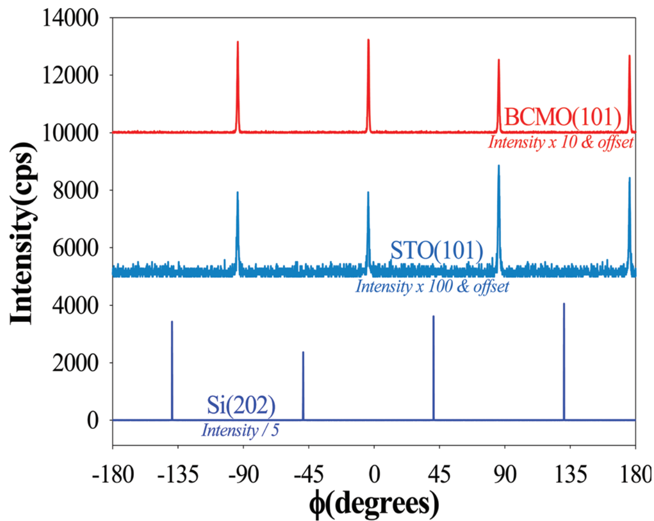

FIG. 6. (Color online) X-ray φ scans of the BCMO(101), STO(101) and Si(202) in the sample with ~8500 Å STO confirm the epitaxial arrangement of the c-axis aligned layers of BCMO and STO (see also Fig. 4).

Each of the φ scans shows only four peaks from the BCMO$\{101\}_{psuedocubic}$, STO{101}, and Si{202} family of planes, respectively, as expected. The alignment between the STO{101} and BCMO{101} family of planes is also expected. The 45° off-set between the Si{202} family of planes and the others is consistent with the 45° difference between the $\langle 100\rangle_{Si}$ and the $\langle 110\rangle_{Si}$ directions. Thus, the φ scans shown in Fig. 5 confirm the expected crystalline epitaxial orientations represented in Fig. 5.

B. Photoinduced effects

Temperature dependence of resistivity of BCMO thin film grown on silicon with a total of ~8500 Å STO buffer layer is shown in Fig. 7. Typically, the temperature dependence of the resistivity of CO materials has a kink (change in derivative) at the CO temperature.[16] However, this feature is less pronounced or almost indistinguishable in thin films,[9,17] and the temperature of transition to a CO state is difficult to determine from resistivity measurement alone. Substrate induced strain is a probable reason for less distinct CO transitions.[18] The resistivity temperature dependence of thin film BCMO on STO buffered silicon similar to BCMO on STO does not show this feature below room temperature (Figs. 7 and 8). The charge ordering temperature of BCMO on STO is above room temperature.[9]

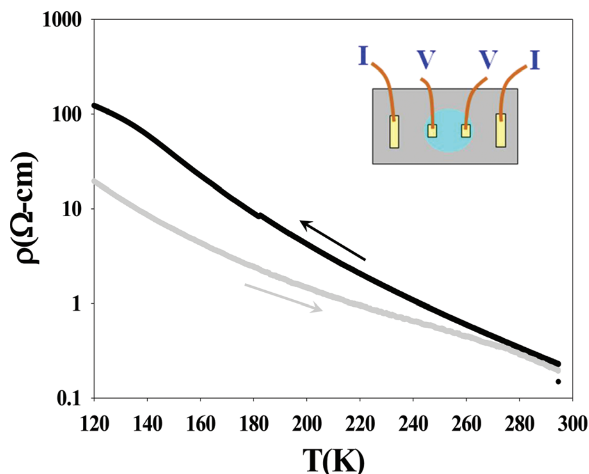

FIG. 7. (Color online) Temperature dependence of the resistivity of BCMO grown on Si with ~8500 Å layer of STO without (black curve) and with (gray curve) laser illumination. Cooling and warming are shown with arrows. These measurements were performed with 10^{-8} A current. The inset shows the arrangement of the four-in-line electrical contacts with the laser spot covering the area in between the two voltage leads.

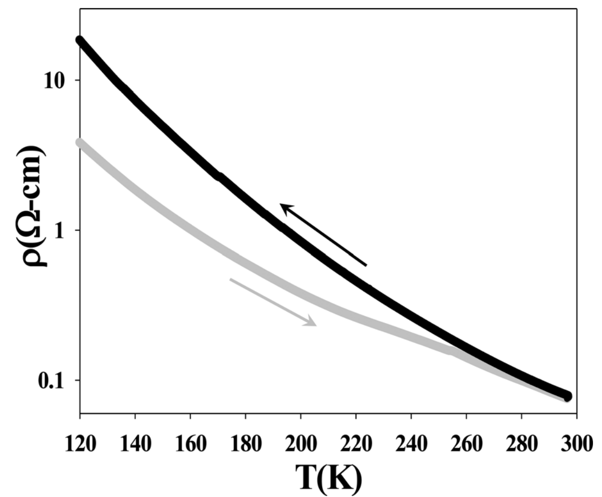

FIG. 8. Temperature dependence of the resistivity of BCMO grown on STO without (black curve) and with (gray curve) laser illumination. Cooling and warming are shown with arrows.

When the film was illuminated with laser light at 120 K, resistivity decreased almost 1 order of magnitude and remained lower than the value of resistivity without illumination for warming up to 275 K (Fig. 7). This behavior is very similar to that of BCMO on $SrTiO_3$ (Fig. 8). Photoinduced changes in this material are associated with melting of charge ordering by light.[9,19]

As light partially destroys the CO resistivity of the material decreases, and when the illumination is switched off, resistivity recovers its original value. Figure 9(a) shows the time dependence of resistivity at 160 K after the illumination was switched on and off. Similar behavior is observed at temperatures below the CO temperature (~275 K). These time dependencies can be fitted to the exponential law: $\Delta R \propto \exp(-t/\tau)$. Figure 9(b) shows the temperature dependence of the time constants τ_1 and τ_2 of exponential decrease/increase after the illumination was switched on or off. Time constants are of the order of 1 min. Time constants associated with transition to more conductive state are shorter than time constants associated with transition from light induced conductive state to original state. This light induced resistivity changes and its dynamics are similar to that observed in BCMO films grown on oxide substrates.[8,9]

IV. CONCLUSIONS

We have achieved epitaxial growth of BCMO thin films on STO buffered silicon. We found that the optimal temperature for growing epitaxial BCMO films on STO buffered silicon is 750 °C. Thin film of BCMO on STO buffered silicon

Downloaded 18 Apr 2011 to 129.2.19.99. Redistribution subject to AIP license or copyright; see http://jap.aip.org/about/rights_and_permissions

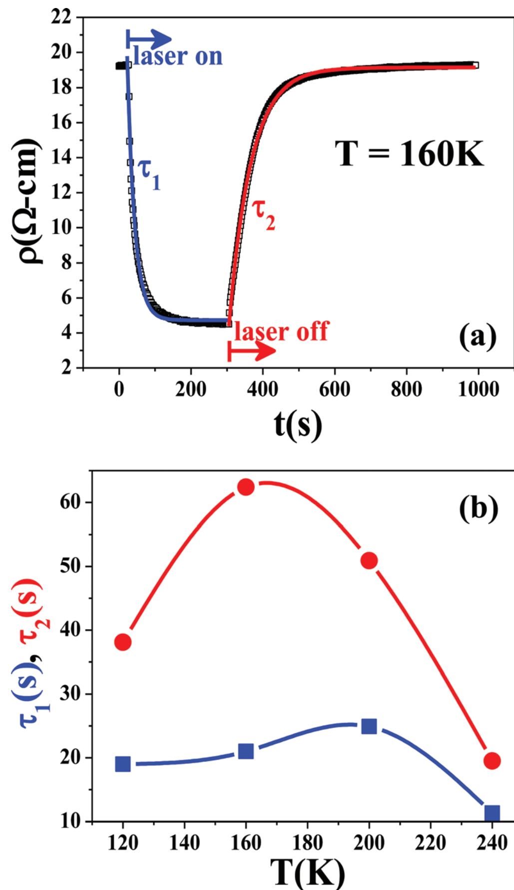

FIG. 9. (Color online) (a) Change of resistivity with time of BCMO grown on ~8500 Å STO after laser illumination was switched on and off at T = 160 K. Blue and red solid lines represent fits to the exponential time dependence $\Delta R \propto \exp(-t/\tau)$. (b) Temperature dependence of the time constants of exponential decrease of resistivity after the laser illumination was switched on (squares) and exponential increase of resistivity after illumination was switched off (circles). Solid lines are guides for an eye.

exhibit significant photoinduced resistivity changes (up to 1 order of magnitude at 120 K). The lifetime of photoinduced conductive state is on the order of 1 min. This photoresponse and its dynamics are similar to that of BCMO films on oxide substrates.[8,9]

ACKNOWLEDGMENTS

This work is supported by NSF grant DMR-0348939. We acknowledge support from the undergraduate research grants to Benjamin Hofmann from the Jess and Mildred Fisher College of Science and Mathematics, Towson University. Thanks are due to Jeff Klupt for experimental help.

[1] I. I. Smolyaninov, V. N. Smolyaninova, C. C. Davis, S.-W. Cheong, and R. L. Greene, Phys. Rev. Lett. **87**, 127204 (2001).

[2] V. A. Bokov, N. A. Grigorian, and M. F. Bryzhina, Phys. Status Solidi **20**, 745 (1967).

[3] S. A. Campbell, *Fabrication Engineering at the Micro and Nanoscale*, 3rd ed. (Oxford University Press, USA, 2008); J.-H. Kim and A. M. Grishin, Integr. Ferroelectr. **80**, 47 (2006).

[4] K. Eisenbeiser, R. Droopad, Z. Yu, C. Overgaard, J. Kulik, J. Finder, S. M. Smith, S. Voight, and D. Penunuri, J. Electron. Mater. **32**, 868 (2003); J. Lettieri, J. H. Haeni, and D. G. Schlom, J. Vac. Sci. Technol. A **20**, 1332 (2002); H. Li, X. Hu, Y. Wei, Z. Yu, X. Zhang, R. Droopad, A. A. Demkov, J. Edwards, Jr., K. Moore, W. Ooms, J. Kulik, and P. Fejes, J. Appl. Phys. **93**, 4521 (2003); G. Y. Yang, J. M. Finder, J. Wang, Z. L. Wang, Z. Yu, J. Ramdani, R. Droopad, K. W. Eisenbeiser, and R. Ramesh, J. Mater. Res. **17**, 204 (2002); Z. Yu, Y. Liang, C. Overgaard, X. Hu, J. Curless, H. Li, Y. Wei, B. Craigo, D. Jordan, R. Droopad, J. Finder, K. Eisenbeiser, D. Marshall, K. Moore, J. Kulik, and P. Fejes, Thin Solid Films 462–463, 51 (2004).

[5] Y. Liang, Y. Wei, X. M. Hu, Z. Yu, R. Droopad, H. Li, and K. Moore, J. Appl. Phys. **96**, 3413 (2004); R. Droopad, Z. Yu, H. Li, Y. Liang, C. Overgaard, A. Demkov, X. Zhang, K. Moore, K. Eisenbeiser, M. Hu, J. Curless, and J. Finder, J. Cryst. Growth **251**, 638 (2003).

[6] Y. Liang, S. Gan, and M. Engelhard, Appl. Phys. Lett. **79**, 3591 (2001).

[7] X. Hu, H. Li, Y. Liang, Y Wei, Z. Yu, D. Marshall, J. Edwards, Jr., R. Droopad, X. Zhang, A. A. Demkov, K. Moore, and J. Kulik, Appl. Phys. Lett. **82**, 203 (2003).

[8] V. N. Smolyaninova, M. Rajeswari, R. Kennedy, M. Overby, S. E. Lofland, L. Z. Chen, and R. L. Greene, Appl. Phys. Lett. **86**, 071922 (2005).

[9] V. N. Smolyaninova, E. Talanova, R. Kennedy, Rajeswari M. Kolagani, M. Overby, L. Aldaco, G. Yong, and K. Karki, Phys. Rev. B **76**, 104423 (2007).

[10] V. N. Smolyaninova, G. Yong, R. M. Kolagani, K. Karki, and B. Hofmann, J. Appl. Phys. **106**, 043902 (2009).

[11] G. J. Yong, Rajeswari M. Kolagani, S. Adhikari, R. M. Mundle, D. W. Cox, A. L. Davidson III, Y. Liang, O. B. Drury, S. P. Hau-Riege, C. Gardner, E. Ables, R. M. Bionta, and S. Friedrich, Sens. Lett. **6**, 741 (2008).

[12] G. J. Yong, R. M. Kolagani, S. Adhikari, O. B. Drury, C. Gardner, R. M. Bionta, and S. Friedrich, Rev. Sci. Instrum. **81**, 113906 (2010).

[13] PDF files: $TiSi_2$ # 35-0785 and $SrSiO_3$ # 30-1302.

[14] G. J. Yong, Rajeswari M. Kolagani, S. Adhikari, W. Vanderlinde, Y. Liang, K. Muramatsu, and S. Friedrich, J. Appl. Phys. **108**, 033502 (2010).

[15] M. Rajeswari, R. Shreekala, A. Goyal, S. E. Lofland, S. M. Bhagat, K. Ghosh, R. P. Sharma, R. L. Greene, R. Ramesh, T. Venkatesan, and T. Boettcher, Appl. Phys. Lett. **73**, 2672 (1998).

[16] H. Woo, T. A. Tyson, M. Croft, S.-W. Cheong, and J. C. Woicik, Phys. Rev. B **63**, 134412 (2001).

[17] S. Chaudhuri and R. C. Budhani, Phys. Rev. B **74**, 054420 (2006).

[18] D. H. Kim, H. M. Christen, M. Varela, H. N. Lee, and D. H. Lowndes, Appl. Phys. Lett. **88**, 202503 (2006).

[19] C. S. Nelson, R. M. Kolagani, M. Overby, V. N. Smolyaninova, and R. Kennedy, J. Phys.: Condens. Matter **18**, 997 (2006).

Downloaded 18 Apr 2011 to 129.2.19.99. Redistribution subject to AIP license or copyright; see http://jap.aip.org/about/rights_and_permissions